Dear Sébastian,

Thank you for going through the referee's comments and for your additional suggestions. You suggested to include soil type in the figure labeling and to clarify the counterintuitive turnover pattern in the Podzol. We have **incorporated** them:

(1) **In the figures, we have now included both the soil type and location.** We have also taken the opportunity to improve the colour scheme of Figure 4.

(2) **Thank you for highlighting the Podzol dynamics.** Indeed, you are right. Oxides and hydroxides are crucial for stabilization, so higher C dynamics in the deep soil versus the shallower soil is counterintuitive. We did not sufficiently explain the pedogenetic horizons in the Podzol in order to explain the pattern. The crux is the transition from the elluvial to the illuvial horizon. We have now corrected this.
In detail:
The elluvial horizon in Beatenberg extends from 4-5 cm downwards up to ~35 cm. The illuviation leeches the iron, aluminium out of the soil layer. Deeper, in the illuviation horizon (~35-60 cm), there is a redeposition of iron and aluminium which stabilizes the organic matter.
The counterintuitive pattern that you correctly noted is that in the shallower 20-40 cm layer - which encompasses the elluvial horizon – the turnover is slower than the deeper (40-60) layer - which encompasses the illuvial soil horizon. The reason the counter-intuitive pattern occurs is that elluvial horizon (mostly represented in the 20-40 layer) there are lower amounts of oxydes and hydroxydes as compared to the deeper layers. In the deeper layer (40-60), the organic matter can form organo-mineral complexes again and the carbon dynamics are faster.

Thank you very much again, we look forward to the feedback of the referees,

Tessa

Dynamics of deep soil carbon – insights from ^{14}C time-series across a climatic gradient

Tessa Sophia van der Voort[1], Utsav Mannu[1,†], Frank Hagedorn[2], Cameron McIntyre[1,3], Lorenz Walthert[2], Patrick Schleppi[2], Negar Haghipour[1], Timothy Ian Eglinton[1]

[1]Institute of Geology, ETH Zürich, Sonneggstrasse 5, 8092 Zürich, Switzerland
[2]Forest soils and Biogeochemistry, Swiss Federal Research Institute WSL, Zürcherstrasse 111, 8903 Birmensdorf, Switzerland
[3]Department of Physics, Laboratory of Ion Beam Physics, ETH Zurich, Schaffmattstrasse 20, 9083 Zurich
[†]New address: Department of Earth and Climate Science, IISER Pune, Pune, India

correspondence to: Tessa Sophia van der Voort (tessa.vandervoort@erdw.ethz.ch)

Abstract. Quantitative constraints on soil organic matter (SOM) dynamics are essential for comprehensive understanding of the terrestrial carbon cycle. Deep soil carbon is of particular interest, as it represents large stocks and its turnover rates remain highly uncertain. In this study, SOM dynamics in both the top and deep soil across a climatic (average temperature ~1-9 °C) gradient are determined using time-series (~20 years) ^{14}C data from bulk soil and water-extractable organic carbon (WEOC). Analytical measurements reveal enrichment of bomb-derived radiocarbon in the deep soil layers on the bulk level during the last two decades. The WEOC pool is strongly enriched in bomb-derived carbon, indicating that it is a dynamic pool. Turnover time estimates of both the bulk and WEOC pool show that the latter cycles up to a magnitude faster than the former. The presence of bomb-derived carbon in the deep soil, as well as the rapidly turning WEOC pool across the climatic gradient implies that there likely is a dynamic component of carbon in the deep soil. Precipitation and bedrock type appear to exert a stronger influence on soil C turnover and stocks as compared to temperature.

1 Introduction

Within the broad societal challenges accompanying climate and land use change, a better understanding of the drivers of turnover of carbon in the largest terrestrial reservoir of organic carbon, as constituted by soil organic matter (SOM), is essential (Batjes, 1996; Davidson and Janssens, 2006; Doetterl et al., 2015; Prietzel et al., 2016). Terrestrial carbon turnover remains one of the largest uncertainties in climate model predictions (Carvalhais et al., 2014; He et al., 2016). At present, there is no consensus on the net effect that climate and land use change will have on SOM stocks (Crowther et al., 2016; Gosheva et al., 2017; Melillo et al., 2002; Schimel et al., 2001; Trumbore and Czimczik, 2008). Deep soil carbon is of particular interest because of its large stocks (Jobbagy and Jackson, 2000; Balesdent et al., 2018; Rumpel and Kogel-Knabner, 2011) and perceived stability. The stability is indicated by low ^{14}C content (Rethemeyer et al., 2005; Schrumpf et al., 2013; van der Voort et al., 2016) and low microbial activity (Fierer et al., 2003). Despite its importance, deep soil carbon has been sparsely studied and remains poorly understood (Angst et al., 2016; Mathieu et al., 2016; Rumpel and Kogel-Knabner, 2011). The inherent complexity of SOM and the multitude of drivers controlling its stability further impedes the understanding of this globally significant carbon pool (Schmidt et al., 2011). In this framework, there is a particular interest in the portion of soil carbon that could be most vulnerable to change, especially in colder climates (Crowther et al., 2016). Water-exactable organic carbon (WEOC) is seen as a dynamic and potentially vulnerable carbon pool in the soil (Hagedorn et al., 2004; Lechleitner et al., 2016). Radiocarbon (^{14}C) can be a powerful tool to determine the dynamics of carbon turnover over decadal to millennial timescales

because of the incorporation of bomb-derived ^{14}C introduced in the atmosphere in the 1950's as well as the radioactive decay of ^{14}C naturally present in the atmosphere (Torn et al., 2009). Furthermore, ^{14}C can also be employed to identify petrogenic (or geogenic) carbon in the soil profile. Understanding the potential mobilization of stabilized petrogenic carbon is key because it could constitute an additional CO_2 source to the atmosphere (Hemingway et al., 2018). Time-series ^{14}C data is particularly insightful because it enables the tracking of recent decadal carbon. Furthermore, single time-point ^{14}C data can yield two estimates for turnover time, whilst time-series data yields a single turnover estimate (Torn et al., 2009). Given that the so-called "bomb radiocarbon spike" will continue to diminish in the coming decades, time-series measurements are increasingly a matter of urgency in order to take full advantage of this intrinsic tracer (Graven, 2015). Several case-studies have collected time-series ^{14}C soil datasets and demonstrated the value of this approach (Baisden and Parfitt, 2007; Prior et al., 2007; Fröberg et al., 2010; Mills et al., 2013, Schrumpf and Kaiser, 2015). However, these studies are sparse, based on specific single sites and have been rarely linked to abiotic and biotic parameters. Much more is yet to be learned about the carbon cycling through time-series observations in top- and subsoils along environmental gradients. Furthermore, to our knowledge, there are no studies with pool-specific ^{14}C soil time-series focusing on labile carbon.

This study assesses two-pool soil carbon dynamics as determined by time-series (~20 years) radiocarbon across a climatic gradient. The time-series data is analyzed by a numerically optimized model with a robust error reduction to yield carbon turnover estimates for the bulk and dynamic WEOC pool. Model output is linked to potential drivers such as climate, forest productivity and physico-chemical soil properties. The overall objective of this study is to improve our understanding of shallow and deep soil carbon dynamics in a wide range of ecosystems.

2 Materials and methods

2.1 Study sites, sampling strategy and WEOC extraction

The five sites investigated in this study are located in Switzerland between 46-47° N and 6-10° E and encompass large climatic (mean annual temperature (MAT) 1.3-9.2°C, mean annual precipitation (MAP) 864-2126 mm $m^{-2}y^{-1}$) and geological gradients (Table 1). The sites are part of the Long-term Forest Ecosystem Research program (LWF) at the Swiss Federal Institute for Forest, Snow and Landscape Research, WSL (Schaub et al., 2011; Etzold et al., 2014). The soils of these sites were sampled between 1995 and 1998 (Walthert et al., 2002, 2003) and were re-sampled following the same sampling strategy in 2014 with the aim to minimize noise caused by small-scale soil heterogeneity. In both instances sixteen samples were taken on a regular grid on the identical 43 by 43 meters (~1600 m^2) plot (Fig. 1; see Van der Voort et al., 2016 for further details). For the archived samples taken between 1995 and 1998, mineral soil samples down to 40 cm depth (intervals of 0-5, 5-10, 10-20 and 20-40 cm) were taken on an area of 0.5 by 0.5 m (0.25 m^2). For samples >40 cm (intervals of 40-60, 60-80 and 80-100 cm), corers were used to acquire samples (n=5 in every pit, area ~2.8×10^{-3} m^2). The organic layer was sampled by use of a metal frame (30×30 cm). The samples were dried at 35-40°C, sieved to remove coarse material (2 mm), and stored in hard plastic containers under controlled climate conditions in the "Pedothek" at WSL (Walthert et al., 2002). For the samples acquired in 2014 the same sampling strategy was followed, and samples were taken on the exact same plot proximal (~10 m) to the legacy

84 samples. For the sampling, a SHK Martin Burch AG HUMAX soil corer (~2×10^{-3} m^2) was used for all depths
85 (0-100 cm). For the organic layer, a metal frame of 20×20 cm was used to sample. Samples were sieved (2 mm),
86 frozen and freeze-dried using an oil-free vacuum-pump powered freeze dryer (Christ, Alpha 1-4 LO *plus*). For
87 the time-series radiocarbon measurements, all samples covering ~1600 m^2 were pooled to one composite sample
88 per soil depth using the bulk-density. In order to determine bulk-density of the fine earth of the 2014 samples,
89 stones > 2 mm were assumed to have a density of 2.65 g/cm^3. For the Alptal site, sixteen cores were taken on a
90 slightly smaller area (~1500 m^2) which encompasses the control plot of a nitrogen addition experiment
91 (NITREX project) (Schleppi et al., 1998). For this site, no archived samples are available and thus only the 2014
92 samples were analyzed. Soil carbon stocks were estimated by multiplying SOC concentrations with the mass of
93 soil calculated from measured bulk densities and stone contents for each depth interval (Gosheva et al., 2017).
94 For the Nationalpark site, the soil carbon stocks from 80-100 cm were estimated using data from a separately
95 dug soil profile (Walthert et al., 2003) because the HUMAX corer could not penetrate the rock-dense soil below
96 80 cm depth. In order to understand very deep soil carbon dynamics (i.e. >100 cm), this study also includes
97 single-time point ^{14}C analyses of soil profiles that were dug down to the bedrock between 1995 and 1998 as part
98 of the LWF programme on the same sites (Walthert et al., 2002). The sampling of the profiles has not yet been
99 repeated.
100
101 **2.2 Climate and soil data**
102 Temperature and precipitation data are derived from weather stations close to the study sites that have been
103 measuring for over two decades, yielding representative estimates of both variables and over the time period
104 concerned in this study (Etzold et al., 2014). The pH values for all sites and concerned depth intervals were
105 acquired during the initial sampling campaign (Walthert et al. 2002). At Alptal, pH values were determined as
106 described in Xu et al. (2009), values of 10-15 cm were extrapolated to the deeper horizons because of the
107 uniform nature of the Gley horizon. The Beatenberg Podzol is marked by strong elluviation (~4-35 cm) and
108 illuviation (~35-60 cm) (Walthert et al., 2003). Exchangeable cations were extracted (in triplicate) from the 2-
109 mm-sieved soil in an unbuffered solution of 1 M NH_4Cl for 1 hour on an end-over-end shaker using a soil-to-
110 extract ratio of 1:10. The element concentrations in the extracts were determined by inductively coupled plasma
111 atomic emission spectroscopy (ICP-AES) (Optima 3000, Perkin–Elmer). Contents of exchangeable protons
112 were calculated as the difference between the total and the Al-induced exchangeable acidity as determined (in
113 duplicate) by the KCl method (Thomas, 1982). This method was applied only to soil samples with a pH ($CaCl_2$)
114 < 6.5. In samples with a higher pH, we assumed the quantities of exchangeable protons were negligible. The
115 effective cation-exchange capacity (CEC) was calculated by summing up the charge equivalents of
116 exchangeable Na, K, Mg, Ca, Mn, Al, Fe and H. The base saturation (BS) was defined as the percental fraction
117 of exchangeable Na, K, Mg, and Ca of the CEC (Walthert et al., 2002, 2013). Net primary production (NPP)
118 was determined by Etzold et al. (2014) as the sum of carbon fluxes by woody tree growth, foliage, fruit
119 production and fine root production. Soil texture (sand, silt and clay content) on plot-averaged samples taken in
120 2014 have been determined using grain size classes for sand, silt and clay respectively of 0.05-2 mm, 0.002-0.05
121 mm and <0.002 mm according to Klute (1986). The continuous distribution of grain sizes was also determined
122 after removal of organic matter (350 °C for 12 h) using the Mastersizer 2000 (Malvern Instruments Ltd.). Soil
123 water potential (SWP) was measured on the same sites as described in Von Arx et al., (2013). In accordance

Comment [TSvdV1]: Dear Sébastian, we included more detail regarding the Beatenberg Podzol soil horizons.

with Mathieu et al., (2015), topsoil refers to the mineral soil up to 20 cm depth, and deep soil refers to mineral soil below 20 cm. Out of the five sites, two are hydromorphic (Gleysol and Podzol in Alptal and Beatenberg respectively), whilst the others are non-hydromorphic (Luvisol, Cambisol and Fluvisol in Othmarsingen, Lausanne and Nationalpark respectively).

2.3 Isotopic (^{14}C, ^{13}C) and compositional (C, N) analysis

Prior to the isotopic analyses, inorganic carbon in all samples was removed by vapour acidification for 72 hours (12M HCl) in desiccators at 60 °C (Komada et al., 2008). After fumigation, the acid was neutralised by substituting NaOH pellets for another 48 hours. All glassware used during sample preparation was cleaned and combusted at 450°C for six hours prior to use. Water extractable organic carbon (WEOC) was procured by extracting dried soil with of 0.5 wt% pre-combusted NaCl in ultrapure Milli-Q (MQ) water in a 1:4 soil:water mass ratio (adapted from Hagedorn et al., (2004), details in Lechleitner et al., (2016)).

In order to determine absolute organic carbon and nitrogen content as well as ^{13}C values, an Elemental Analyser-Isotope Ratio Mass Spectrometer system was used (EA-IRMS, Elementar, vario MICRO cube – Isoprime, Vison). Atropine (Säntis) and an in-house standard peptone (Sigma) were used for the calibration of the EA-IRMS for respectively carbon concentration, nitrogen concentration and C:N ratios and ^{13}C. High ^{13}C values were used to flag if all inorganic carbon had been removed by acidification.

For the ^{14}C measurements of the bulk soil samples were first graphitised using an EA-AGE (elemental analyser-automated graphitization equipment, Ionplus AG) system at the Laboratory of Ion Beam Physics at ETH Zürich (Wacker et al., 2009). Graphite samples were measured on a MICADAS (MIniturised radioCArbon DAting System, Ionplus AG) also at the Laboratory of Ion Beam Physics, ETH Zürich (Wacker et al., 2010). For three samples (Alptal depth intervals 40-60, 60-80 and 80-100 cm) the ^{14}C signature was directly measured as CO_2 gas using the recently developed online elemental analyzer (EA) - stable isotope ratio mass spectrometers (IRMS)–AMS system et ETH Zürich (McIntyre et al., 2016). Oxalic acid (NIST SRM 4990C) was used as the normalising standard. Phthalic anhydride and in-house anthracite coal were used as blank. Two in-house soil standards (Alptal soil 0-5 cm, Othmarsingen soil 0-5 cm) were used as secondary standards. For the WEOC, samples were converted to CO_2 by Wet Chemical Oxidation (WCO) (Lang et al., 2016) and run on the AMS using a Gas Ion Source (GIS) interface (Ionplus). To correct for contamination, a range of modern standards (sucrose, Sigma, $\delta 13C$ = -12.4 ‰ VPDB, $F^{14}C$ = 1.053 ± 0.003) and fossil standards (phthalic acid, Sigma, $\delta 13C$ = -33.6‰ VPDB, $F^{14}C$ <0.0025) were used (Lechleitner et al., 2016).

2.4 Numerical optimization to find carbon turnover and size of the dynamic pool

2.4.1 Turnover based on a single ^{14}C measurement

The ^{14}C signature of a sample can be used to estimate turnover time of a carbon pool (Torn et al., 2009).

$$R_{sample,t} = k \times R_{atm,t} + (1 - k - \lambda) \times R_{sample(t-1)} \quad (1)$$

$$R_{sample,t} = \frac{\Delta^{14}C_{sample}}{1000} + 1 \quad (2)$$

In Eq. 1-2, the constant for radioactive decay of ^{14}C is indicated as λ, the decomposition rate k (inverse of turnover time) is the only unknown in this equation and is hence the variable for which the optimal value that fits the data is sought using the model. The R value of the sample is inferred from $\Delta^{14}C$, hence accounting for the sampling year, as shown in Eq. (2) (Herold et al., 2014; Solly et al., 2013). In order to avoid ambiguity, the term *turnover time* and not i.e. mean residence time is used solely in this manuscript (Sierra et al., 2016).

For the turnover time estimation, we assumed the system to be in steady state over the modeled period (~1×10^4 years, indicating soil formation since the last glacial retreat (Ivy-Ochs et al., 2009)), hence accounting both for radioactive decay and incorporation of the bomb-testing derived material produced in the 1950's and 1960's (Eq. 1.) (Herold et al., 2014; Torn et al., 2009). We assumed an initial fraction modern (F_m) of ^{14}C value of 1 at 10000 B.C.. For the period after 1900 atmospheric fraction modern (F_m) values of the Northern Hemisphere were used (Hua et al., 2013). This equation could be solved in Excel with manual iterations (e.g. Herold et al., 2014), or alternatively a numerical optimization can be used to find the best fit automatically. In this paper, we used a numerical optimization constructed in MATLAB version 2015a (The MathWorks, Inc., Natick, Massachusetts, United States) to find the best fit. The numerical optimization is exhaustive, meaning that every single turnover value from 1 to 10.000 years with an interval of 0.1 year is tested. The error is defined as the difference between the fitted value of R and the measured value (Eq. 3). The turnover value with the lowest error is then automatically selected.

$$Error_{single\ timepoint} = |R_{calculated} - R_{measured}| \quad (3)$$

The residual error of each fit are provided in the Supplemental Information (SI) Table 3. Turnover times determined with the numerical optimization match the manually optimized turnover modeling published previously (Herold et al., 2014; Solly et al., 2013).

2.4.2 Turnover based on two ^{14}C measurements

A single ^{14}C value could yield possible turnover values (Torn et al., 2009, Graven et al., 2015). If there is a time-series ^{14}C dataset, this problem can be eliminated. In this paper, we have time-series data of both the bulk soil, as well as the vulnerable fraction (WEOC). For all samples a time-series dataset is available, both data points are employed to give the best estimate of turnover time. The same numerical optimization (Eq. 1 and 2) as we did for a single time-point, except that we try to find the best fit for both time points whilst reducing the compounding residual mean square error (RSME, Eq. 4). As can be seen in Fig. 2a, single time points can yield

two likely turnover times but when two datapoints are available, a single value can be found. The input data for Figure 2 can be found in SI Table 1. The results of the time-series turnover modelling for both the bulk and WEOC pool of the sub-alpine site Beatenberg are shown in Fig. 3.

$$Error_{two\ timepoints} = \sqrt[2]{|R_{calculated} - R_{measured}|^2_{time\ point\ 1} + |R_{calculated} - R_{measured}|^2_{time\ point\ 1}} \quad (4)$$

2.4.3 Vegetation-induced lag

In order to account for vegetation-lag, two scenarios were run: firstly (1) with no assumed lag between the fixation of carbon from the atmosphere and input into to the soil and (2) model run with a lag of fixation of the atmospheric carbon as inferred from the dominant vegetation (Von Arx et al., 2013; Etzold et al., 2014). In the case of full deciduous trees coverage a lag of two years was assumed, and for the case of 100% conifer-dominated coverage a lag of 8 years was incorporated (Table 1).

2.4.4 Turnover and size vulnerable pool based on two-pool model

As SOM is complex and composed of a continuum of pools with various ages (Schrumpf and Kaiser, 2015) and there is data available from two SOM pools, the ^{14}C time-series data can be leveraged to create a two-pool model. The following assumptions were made: First, both pools (slow & fast) make up the total carbon pool (Eq. 5). Secondly, the total turnover of the bulk soil is made up out of the "dynamic" fraction turnover multiplied by "dynamic" fraction pool size and the "slow" pool turnover multiplied by "slow" pool size (Eq. 6). Furthermore, we assume that the signature of the sample (the time-series bulk data) is determined by the rate of incorporation of the material (atmospheric signal) and the loss of carbon the two pools (Eq. 7). Lastly, we assume that the radiocarbon signal of the WEOC pool is representative for a dynamic pool, as it could be representative for a larger component of rapidly turning over carbon, even in the deep soil (Baisden and Parfitt, 2007; Koarashi et al., 2012). The turnover rate of the slow pool was set between 100 and 10.000 years, with a time-step of 10 years. The size of the dynamic pool was set to be between 0 and 0.5, with a size-step of 0.01.

$$1 = F_1 + F_2 \quad (5)$$

$$k_{total} = (F_1/k_1 + F_2/k_2)^{-1} \quad (6)$$

$$R_{sample,t} = k_{total} \times R_{atm,t} + F_1[(1 - k_1 - \lambda) \times R_{sample(t-1)}] + F_2(1 - k_2 - \lambda) \times R_{sample(t-1)} \quad (7)$$

Where F_1 is the relative size of the dynamic pool, and F_2 is the relative size of the (more) stable pool. The $k_1$is the inverse of the turnover time of the dynamic or WEOC as determined using the numerical optimisation of Eq. 1-4. The k_2 is the inverse of the turnover time of the slow pool. The calculation of the error term becomes for complex because it needs to be recalculated for each unique combination of pool-size distribution (Eq. 5) and turnover time (inverse of *k*, Eq. 6). Therefore, the error space changes from column vector to a two-dimensional

matrix of length of the step size increments (F_1) and width of the inverse of the turnover time of the slow pool (k_2).

$$Error_{k_2,F_1} = \sqrt[2]{|R_{calculated} - R_{measured}|^2_{time\ point\ 1} + |R_{calculated} - R_{measured}|^2_{time\ point\ 2}} \quad (8)$$

$$Error = Min(Error_{k_2,F_1}) \quad (9)$$

The numerical optimization finds the likeliest solution for the given dataset. This model constitutes a best fit, and more data would better constrain the results. Additional details can be found in the Supplementary Information (SI) text and SI Fig. 1. **All Matlab-based numerical optimization codes can be found in the SI**. For correlations (packages HMISC, corrgram, method = pearson), statistical software R version 1.0.153 was used.

3 Results

3.1 Changes of radiocarbon signatures over time

Overall, there is a pronounced decrease in radiocarbon signature with soil depth at all sites (Fig. 4). The time-series results show clear changes in radiocarbon signature over time from the initial sampling period (1995-1998) as compared to 2014, with the magnitude of change depending on site and soil depth. In the uppermost 5 cm of soils, the overarching trend in the bulk soil is a decrease in the ^{14}C bomb-spike signature in the warmer climates (Othmarsingen, Lausanne), whilst at higher elevation (colder) sites (Beatenberg, Nationalpark) the bomb-derived carbon appears to enter the top soil between 1995-8 and 2014.

Water-extractable OC (WEOC) has an atmospheric ^{14}C signature in the top soil at all sites in 2014. The deep soil in the 1990's still has a negative $\Delta^{14}C$ signature of WEOC at multiple sites. There are two distinguishable types of depth trends for WEOC in the 2014 dataset: (1) WEOC has the same approximate ^{14}C signature throughout depth (Othmarsingen, Beatenberg), (2) WEOC becomes increasingly ^{14}C depleted with depth (Alptal, Nationalpark), or an intermediate form where WEO^{14}C is modern throughout the top soil but becomes more depleted of ^{14}C in the deep soil (Lausanne) (Fig. 4). The isotopic trends of WEOC co-vary with grain size as inherited from the bedrock type (Walthert et al., 2003). Soils with a relatively modern WEO^{14}C signature in 2014 (down to 40 cm) are underlain by bedrock with large grained (SI Fig. 2, Table SI 3) components (the moraines and sandstone at Othmarsingen, Lausanne and Beatenberg respectively). Soils where WEO^{14}C signature decreases with depth are underlain by bedrock containing fine-grained components. For instance, the Flysch in Alptal (Schleppi et al., 1998) and intercalating layers of silt and coarse grained alluvial fan in Nationalpark (Walthert et al., 2003) respectively.

3.2 Carbon turnover patterns

Incorporation of a vegetation-induced time lag (Table 2, SI Table 2) has an effect on modelled carbon dynamics in the organic layer, but this effect is strongly attenuated in the 0-5 cm layer in the mineral soil and virtually absent for the deeper soil layers. The residual errors associated to the carbon turnover estimates converge to a single point (Figure 2) and are low (i.e. < 0.06 R, SI Tables 3 and 4). Turnover times show two modes of behavior for well-drained soils and hydromorphic soils, respectively. The non-hydromorphic soils

have relatively similar values with decadal turnover times for the 0-5 cm layer, increasing to an order of centuries down to 20 cm depth, and to millenia in deeper soil layers (~980 to ~3940 years at 0.6 to 1 m depth) (Fig. 5). In contrast, the hydromorphic soils are marked by turnover times that are up to an order of magnitude larger, from centennial in top soil to (multi-) millennial in deeper soils. At the Beatenberg Podzol, turnover time in the shallow layer which overlaps with the elluvial horizon is slower (20-40 cm, ~1900 y) than the deepest layer (40-60 cm, ~1300 y), which overlaps with the illuvial horizon (Figure 5, SI Table 5).

Comment [TSvdV2]: As suggested we clarified the turnover pattern in the Podzol

Carbon stocks also show distinct difference between drained and hydromorphic soils with greater stock in the hydromorphic soils (~15 kg C m^{-2} at Beatenberg and Alptal vs. ~ 6 - ~7 kg C m^{-2} at Othmarsingen, Lausanne and Nationalpark, Fig. 5, Table 3)).

The turnover times of the WEOC mimic the trends in the bulk soil but are up to an order of magnitude faster. Considering WEOC turnover in the non-hydromorphic soils only, there is a slight increase in WEOC turnover with decreasing site temperature, but the trend is not significant (SI Table 4). The modeled estimate for dynamic fraction is variable at the surface but decreases towards the lower top soil (from ~0.2 at 0-5 cm to ~0.01 at 10-20 cm in Othmarsingen). In the deep soil, the model indicates there could also be a non-negligible proportion of dynamic carbon (e.g. 0.10-0.23 at 20-40 cm). The residual errors associated to the error reduction of the two-pool model are also low (i.e. < 0.06 R). but do not converge as strongly as the single-pool model (SI Figure 1).

3.3 Pre-glacial carbon in deep soil profiles

The turnover times of deep soil carbon exceed 10,000 years in several profiles, indicating the presence of carbon that pre-dates the glacial retreat (Fig. 6). These profiles are located on carbon-containing bedrock and concern the deeper soil (80-100 cm) of the Gleysol (Alptal), as well as >100 cm in the Cambisol (Lausanne) (Fig. 6, SI Table 6).

3.4 Environmental drivers of carbon dynamics

Pearson correlation was used to assess potential relationships between carbon stocks and turnover and their potential controlling factors (climate, NPP, soil texture, soil moisture and physicochemical properties (Table 4, SI Table 7, 8)). For the averaged top soil (0-20 cm, n=5), carbon stocks were significantly positive correlated to Mean Annual Precipitation (MAP). Turnover time in the bulk top soil negatively correlated with silt content and positively with average grain size. Turnover time in the WEOC of the top soil did not correlate significantly with any parameter except a weak positive correlation with grain size. Deeper soil bulk stock and turnover time positively correlated with MAP and iron content.

4 Discussion

4.1 Dynamic deep soil carbon

4.1.1 Rapid shifts in ^{14}C abundance reflect dynamic deep carbon

The propagation of bomb-derived carbon into supposedly stable deep soil on the bulk level across the climatic gradient implies that SOM in deep soil contains a dynamic pool and could be less stable and potentially more vulnerable to change than previously thought. This possibility is further supported by the WEO^{14}C which is

consistently more enriched in bomb-derived carbon than the bulk soil. Near-atmospheric signature WEO^{14}C pervades up to 40 or even 60 cm depth. Hagedorn et al., (2004) also found WEOC to be a highly dynamic pool using ^{13}C tracer experiments in forest soils.

We consider our ^{14}C comparison over time to be robust because the grid-based sampling and averaging was repeated on the same plots which excludes the effect plot-scale variability (Van der Voort et al., 2016). Our ^{14}C time-series data in the deep soil corroborate pronounced changes in ^{14}C (hence substantial SOM turnover) in subsoils of an area with pine afforestation (Richter and Markewitz, 2001). The findings are also in agreement with results from an incubation study by Fontaine et al., (2007) which showed that the deep soil can have a significant dynamic component. Baisden et al., (2007) also found indications of a deep dynamic pool using modeling on ^{14}C time-series on the bulk level on a New Zealand soil under stable pastoral management.

4.1.2 Carbon dynamics reflect soil-specific characteristics at depth

Bulk carbon turnover for the top and deeper soil fall in the range of prior observations and models, although the data for the latter category is sparse (Scharpenseel and Becker-Heidelmann, 1989; Paul et al., 1997; Schmidt et al., 2011; Mills et al., 2013; Braakhekke et al., 2014). The carbon turnover is related to soil-specific characteristics. The slower turnover of hydromorphic as compared to non-hydromorphic soils is likely due to increased waterlogging and limited aerobicity (Hagedorn et al., 2001) which is conducive to slow turnover and enhanced carbon accumulation. The WEOC turns over up to an order of magnitude faster than the bulk and mirrors these trends, indicating that it indeed is a more dynamic pool (Hagedorn et al., 2004; Lechleitner et al., 2016). Results also reflect known horizon-specific dynamics for certain soil types, particularly in the deep soil. The hydromorphic Podzol at Beatenberg shows specific pedogenetic features such as an illuviation layer with an enrichment in humus and iron in the deeper soil (Walthert et al., 2003) where turnover of bulk and WEOC is faster and stocks are higher as compared to the elluvial layer above (Fig. 5). This is likely due to the input of younger carbon via leaching of dissolved organic carbon. The non-hydromorphic Luvisols are marked by an enrichment of clay in the deeper soil, which can enhance carbon stabilization (Lutzow et al., 2006). This also reflected in the turnover time of the 60-80 cm layer in the Othmarsingen Luvisol – in this clay-enriched depth interval (Walthert et al., 2003), turnover is relatively slow as compared to the other (colder) non-hydromorphic soils (Fig. 5). These patterns are consistent with findings by Mathieu et al., (2015) that the important role of soil pedology on deep soil carbon dynamics.

Comment [TSvdV3]: We have further clarified the Podzol turnover pattern here

4.1.3 Dynamic carbon at depth & implications for carbon transport

The analytical ^{14}C data as well as turnover time estimates indicate that there is likely a dynamic portion of carbon in the deep soil. The estimated size of the dynamic pool can be large, even at greater depth than it was observed by other ^{14}C time-series (Richter and Markewitz, 2001; Baisden and Parfitt, 2007; Koarashi et al., 2012). The two-pool modelling indicates that the size of dynamic pool in the deep soil can be upwards of ~10%. A deep dynamic pool is consistent with findings of a ^{13}C tracer experiment by Hagedorn et al., (2001) that shows with that relatively young (<4 years) carbon can be rapidly incorporated in the top soil (20% new C at 0-20 cm depth) but also in the deep soil (50 cm), and findings by Balesdent et al., (2018) which estimate that up to 21% of the carbon between 30-100 cm is younger than 50 years. Rumpel and Kögel-Knabner (2011) have highlighted the importance of the poorly understood deep soil carbon stocks and a significant dynamic pool in

the deep soil could imply that carbon is more vulnerable than initially suspected. One major input pathway of younger C into deeper soils is the leaching of DOC (Kaiser and Kalbitz, 2012; Sanderman and Amundson, 2009). Here, we have measured WEOC – likely primarily composed of microbial metabolites (Hagedorn et al., 2004) – carrying a younger ^{14}C signature than bulk SOM and thus, representing a translocator of fresh carbon to the deep soil. The WEOC turnover time is in the order of decades, implying that it is not directly derived from decaying vegetation, but rather composed of microbial material feeding on the labile portion of the bulk soil. In addition to WEOC, roots and associated mycorrhizal communities may also provide a substantial input of new C into soils in deeper soils (Rasse et al., 2005). Additional modelling such as in CENTURY and RotC could provide additional insights into the soil carbon dynamics and fluxes (Manzoni et al., 2009)

4.2 Contribution of petrogenic carbon

Our results on deep soil carbon suggest the presence of pre-aged or ^{14}C-dead (fossil), pre-interglacial carbon in the Alptal (Gleysol) and Lausanne (Cambisol) profiles, implying that a component of soil carbon is not necessarily linked to recent (< millenial) terrestrial productivity and instead constitutes part of the long-term (geological) carbon cycle (> millions of years). In the case of the Gleysol in Alptal, the ^{14}C-depleted material could be derived from the poorly consolidated sedimentary rocks (Flysch) in the region (Hagedorn et al., 2001a; Schleppi et al., 1998; Smith et al., 2013), whereas carbon present in glacial deposits and molasse may contribute in deeper soils at the Lausanne (Cambisol) site. The potential contribution of fossil carbon was estimated using a mixing model using the signature of a soil without fossil carbon, the signature of fossil carbon and the measured values (SI Table 4). Fossil carbon contribution in the Alptal profile between 80-100 cm (Fig. 6, SI Table 4) is estimated at ~40 %. Below one meter at Lausanne site the petrogenic percentage ranges from ~20% at 145 cm up to ~80 % at 310 cm depth (Fig. 6, SI Table 4).

Other studies analyzing soils have observed the significant presence of petrogenic (geogenic in soil science terminology) in loess-based soils (Helfrich et al., 2007; Paul et al., 2001). Our results suggest that pre-glacial carbon may comprise a dominant component of deep soil organic matter in several cases, resulting in an apparent increase in the average age (and decrease in turnover) of carbon in these soils. Hemingway et al., (2018) have highlighted that fossil carbon oxidized in soils can lead to significant additional CO_2 emissions. Therefore, the potential of soils to 'activate' fossil petrogenic carbon should be considered when evaluating the soil carbon sequestration potential.

4.3 Controls on carbon dynamics and cycling

In order to examine the effects of potential drivers on soil C turnover and stocks, we explore correlations between a number of available factors which have previously been proposed, such as texture, geology, precipitation, temperature and soil moisture (Doetterl et al., 2015; McFarlane et al., 2013; Nussbaum et al., 2014; Seneviratne et al., 2010; van der Voort et al., 2016).

From examination of data for all samples it emerges that C turnover does not exhibit a consistent correlation with any specific climatological or physico-chemical factor. This implies that no single mechanism predominates and/or that there is a combined impact of geology and precipitation as these soil-forming factors affect grain size distribution, water regime and mass transport in soils. Exploring potential relationships in greater detail, we see that carbon stocks in the top soil and deep soil as well as turnover time is positively related

to MAP, which could be linked to waterlogging and anaerobic conditions even in upland soils leading to a lower decomposition and thus to a higher build-up of organic material (Keiluweit et al., 2015). Our results are supported by the findings based on >1000 forest sites that precipitation exerts a strong effect on soil C stocks across Switzerland (Gosheva et al., 2017; Nussbaum et al., 2014). Furthermore, Balesdent et al., (2008) also highlighted the role of precipitation and evapotranspiration on deep soil organic carbon stabilisation. Nonetheless, it has to be noted that for these sites, the precipitation range does not include very dry soils (MAP 864-2126 mm/y). Turnover in both top and deep soil was most closely correlated with texture. The positive correlation of top soil turnover with grain size and negative correlation with the amount of silt-sized particles reflects lower stabilization in larger-grained soils as opposed to clay-rich soils with a higher and more reactive surface area (Rumpel and Kogel-Knabner, 2011). Mathieu et al., (2015) also stressed the decisive role of soil pedology on deep soil carbon storage. Overall, geology seems to impact the carbon cycling in three key ways. Firstly, when petrogenic carbon is present in the bedrock from shale or reworked shale (Schleppi et al., 1998; Walthert et al., 2003), fossil carbon contributes to soil carbon. Secondly, porosity of underlying bedrock either prevents or induces waterlogging which in turn affects turnover. Thirdly, the initial components of the bedrock (i.e. silt-sizes layers in an alluvial fan) influence the final grain size distribution and mineralogy (SI Fig. 2, Table 3), which is also reflected in the bulk and pool-specific turnover. Within the limited geographic and temporal scope of this paper, we hypothesize that for soil carbon stocks and their turnover, temperature is not the dominant driver, which has been concluded by some (Giardina and Ryan, 2000) but refuted by others (Davidson et al., 2000; Feng et al., 2008). The only climate-related driver which appears to be significant for the deep soil is precipitation.

4.4 Modular robust numerical optimization

The numerical approach used here builds on previous work concerning turnover modeling of bomb-radiocarbon dominated samples (Herold et al., 2014; Solly et al., 2013; Torn et al., 2009) and the approach used in numerous time-series analysis with box modeling using Excel (Schrumpf and Kaiser, 2015) or Excel solver (Baisden et al., 2013; Prior et al., 2007). However certain modifications were made in order to (i) provide objective repeatable estimates, (ii) incorporate longer time-series data, and (iii) identify samples impacted by petrogenic (also called geogenic) carbon. Identifying petrogenic carbon in the deep soil is important considering the large carbon stocks in deep soils (Rumpel and Kogel-Knabner, 2011) and the wider relevance of petrogenically-derived carbon in the global carbon cycle (Galy et al., 2008). This approach is modular and could be adapted in the future to identify the correct turnover for time-series ^{14}C data, which is becoming increasingly important with the falling bomb-peak (Graven, 2015). For the single and time-series data, the results from the numerical solution were benchmarked to the Excel-based model, and it was found that the results agree.

Other studies (e.g. Baisden and Canessa, 2012; Prior et al., 2007) also use time-series data to estimate the value for two unknowns simultaneously (size of the pool size and turnover time). The error does not always converge to single low point, but can have multiple minima (SI Fig. 1). This potential issue should be considered when interpreting the data. More time-series data is required to eliminate this problem.

5 Conclusion

Time-series radiocarbon (^{14}C) analyses of soil carbon across a climatic range reveals recent bomb-derived radiocarbon in both upper and deeper bulk soil, implying the presence of a rapidly turning over pool at depth. Pool-specific time-series measurements of the WEOC indicate this is a more dynamic pool which is consistently more enriched in radiocarbon than the bulk. Furthermore, the estimated modeled size of the dynamic fraction is non-negligible even in the deep soil (~0.1-0.2). This could imply that a component of the deep soil carbon could be more dynamic than previously thought.

The interaction between precipitation and geology appears to be the main control on carbon dynamics rather than site temperature. Carbon turnover in non-hydromorphic soils is relatively similar (decades to centuries) despite dissimilar climatological conditions. Hydromorphic soils have turnover times which are up to an order of magnitude slower. These trends are mirrored in the dynamic WEOC pool, suggesting that in sandy, non-waterlogged (aerobic) soils the transport of relatively modern (bomb-derived) carbon into the deep soil and/or the microbial processing is enhanced as compared to fine-grained waterlogged (anaerobic) soils.

Model results indicate certain soils contain significant quantities of pre-glacial or petrogenic (bedrock-derived) carbon in the deeper part of their profiles. This implies that soils not only sequester "modern" but can rather also mobilize and potentially metabolize "fossil" or geogenic carbon.

Overall, these time-series ^{14}C bulk and pool-specific data provide novel constraints on soil carbon dynamics in surface and deeper soils for a range of ecosystems.

Acknowledgements

We would like to acknowledge the SNF NRP68 *Soil as a Resource* program for funding this project (SNF 406840_143023/11.1.13-31.12.15). We could also like to thank Jerome Balesdent, an anonymous reviewer and the journal editor Sébastian Fontaine for their helpful comments from which this paper greatly benefitted. We could also like to thank Jerome Balesdent, an anonymous reviewer and the journal editor Sébastian Fontaine for their helpful comments from which this paper greatly benefitted. We would like to thank various members of the Laboratory of Ion Beam Physics and Biogeoscience group for their help with the analyses, in particular Lukas Wacker. We thank Roger Köchli for his crucial help in the field which enabled an effective time-series comparison and for his help with subsequent analyses. We thank Emily Solly and Sia Gosheva for their valuable insights, Claudia Zell for her help on the project and in the field, Peter Waldner and Marco Walser for facilitating the fieldwork, and Elisabeth Graf-Pannatier for her insights on soil moisture. The 2014 field campaign would not have been possible without the help of Thomas Blattmann, Lukas Oesch, Markus Vaas and Niko Westphal. Thanks to Stephane Beaussier for the insights into numerical modeling. Also thanks to Nadine Keller and Florian Neugebauer for their help in the lab. Last but not least, thanks to Thomas Bär for summarizing ancillary pH data. Data supporting this paper is provided in a separate data Table.

References

Angst, G., John, S., Mueller, C. W., Kögel-Knabner, I. and Rethemeyer, J.: Tracing the sources and spatial distribution of organic carbon in subsoils using a multi-biomarker approach, Sci. Rep., 6(1), 29478, doi:10.1038/srep29478, 2016.

Von Arx, G., Graf Pannatier, E., Thimonier, A. and Rebetez, M.: Microclimate in forests with varying leaf area index and soil moisture: Potential implications for seedling establishment in a changing climate, J. Ecol., 101(5), 1201–1213, doi:10.1111/1365-2745.12121, 2013.

Baisden, W. T. and Parfitt, R. L.: Bomb 14C enrichment indicates decadal C pool in deep soil?, Biogeochemistry, 85(1), 59–68, doi:10.1007/s10533-007-9101-7, 2007.

Baisden, W. T., Parfitt, R. L., Ross, C., Schipper, L. A. and Canessa, S.: Evaluating 50 years of time-series soil radiocarbon data : towards routine calculation of robust C residence times, Biogeochemistry, 112, 129–137, doi:10.1007/s10533-011-9675-y, 2013.

Batjes, N. H.: Total carbon and nitrogen in the soils of the world, Eur. J. Soil Sci., 47(June), 151–163, 1996.

Balesdent, J., Basile-Doelsch, I., Chadoeuf, J., Cornu, S., Derrien, D., Fekiacova, Z. and Hatté, C.: Atmosphere–soil carbon transfer as a function of soil depth, Nature, 559(7715), 599–602, doi:10.1038/s41586-018-0328-3, 2018.

Braakhekke, M. C., Beer, C., Schrumpf, M., Ekici, A., Ahrens, B., Hoosbeek, M. R., Kruijt, B., Kabat, P. and Reichstein, M.: The use of radiocarbon to constrain current and future soil organic matter turnover and transport in a temperate forest, J. Geophys. Res. Biogeosciences, 119(3), 372–391, doi:10.1002/2013JG002420, 2014.

Carvalhais, N., Forkel, M., Khomik, M., Bellarby, J., Jung, M., Migliavacca, M., Mu, M., Saatchi, S., Santoro, M., Thurner, M., Weber, U., Ahrens, B., Beer, C., Cescatti, A., Randerson, J. T., Reichstein, M., Mu, M., Saatchi, S., Santoro, M., Thurner, M., Weber, U., Ahrens, B., Beer, C., Cescatti, A., Randerson, J. T., Reichstein, M., Mu, M., Saatchi, S., Santoro, M., Thurner, M., Weber, U., Ahrens, B., Beer, C., Cescatti, A., Randerson, J. T. and Reichstein, M.: Global covariation of carbon turnover times with climate in terrestrial ecosystems, Nature, 514(7521), 213–217, doi:10.1038/nature13731, 2014.

Crowther, T., Todd-Brown, K., Rowe, C., Wieder, W., Carey, J., Machmuller, M., Snoek, L., Fang, S., Zhou, G., Allison, S., Blair, J., Bridgham, S., Burton, A., Carrillo, Y., Reich, P., Clark, J., Classen, A., Dijkstra, F., Elberling, B., Emmett, B., Estiarte, M., Frey, S., Guo, J., Harte, J., Jiang, L., Johnson, B., Kröel-Dulay, G., Larsen, K., Laudon, H., Lavallee, J., Luo, Y., Lupascu, M., Ma, L., Marhan, S., Michelsen, A., Mohan, J., Niu, S., Pendall, E., Penuelas, J., Pfeifer-Meister, L., Poll, C., Reinsch, S., Reynolds, L., Schmidth, I., Sistla, S., Sokol, N., Templer, P., Treseder, K., Welker, J. and Bradford, M.: Quantifying global soil C losses in response to warming, Nature, 540(1), 104–108, doi:10.1038/nature20150, 2016.

Davidson, E. A. and Janssens, I. A.: Temperature sensitivity of soil carbon decomposition and feedbacks to climate change., Nature, 440(7081), 165–73 [online] Available from: http://www.ncbi.nlm.nih.gov/pubmed/16525463 (Accessed 28 May 2014), 2006.

Davidson, E. A., Trumbore, S. E. and Amundson, R.: Soil warming and organic carbon content., Nature, 408(December), 789–790, doi:10.1038/35048672, 2000.
Doetterl, S., Stevens, A., Six, J., Merckx, R., Oost, K. Van, Pinto, M. C., Casanova-katny, A., Muñoz, C., Boudin, M., Venegas, E. Z. and Boeckx, P.: Soil carbon storage controlled by interactions between geochemistry and climate, Nat. Geosci., 8(August), 1–4, doi:10.1038/NGEO2516, 2015.
Etzold, S., Waldner, P., Thimonier, A., Schmitt, M. and Dobbertin, M.: Tree growth in Swiss forests between 1995 and 2010 in relation to climate and stand conditions: Recent disturbances matter, For. Ecol. Manage., 311, 41–55 [online] Available from: http://linkinghub.elsevier.com/retrieve/pii/S0378112713003393 (Accessed 3 June 2014), 2014.
Feng, X., Simpson, A. J., Wilson, K. P., Williams, D. D. and Simpson, M. J.: Increased cuticular carbon sequestration and lignin oxidation in response to soil warming, Nat. Geosci., 1(December), 836–839, 2008.
Fierer, N., Schimel, J. P. and Holden, P. A.: Variations in microbial community composition through two soil depth profiles, Soil Biol. Biochem., 35, 167–176, 2003.
Fontaine, S., Barot, S., Barré, P., Bdioui, N., Mary, B. and Rumpel, C.: Stability of organic carbon in deep soil layers controlled by fresh carbon supply., Nature, 450, 277–280, 2007.
Fröberg, M., Tipping, E., Stendahl, J., Clarke, N. and Bryant, C.: Mean residence time of O horizon carbon along a climatic gradient in Scandinavia estimated by 14C measurements of archived soils, Biogeochemistry, 104(1–3), 227–236 [online] Available from: http://link.springer.com/10.1007/s10533-010-9497-3 (Accessed 2 August 2013), 2010.
Galy, V., Beyssac, O., France-Lanord, C. and Eglinton, T. I.: Recycling of graphite during Himalayan erosion: a geological stabilization of carbon in the crust, Science (80-.)., 322(November), 943–945, doi:10.1126/science.1161408, 2008.
Giardina, C. P. and Ryan, M. G.: Evidence that decomposition rates of organic carbon in mineral soil do not vary with temperature, Nature, 404(6780), 858–861, doi:10.1038/35009076, 2000.
Gosheva, S., Walthert, L., Niklaus, P. A., Zimmermann, S., Gimmi, U. and Hagedorn, F.: Reconstruction of Historic Forest Cover Changes Indicates Minor Effects on Carbon Stocks in Swiss Forest Soils, Ecosystems, (C), doi:10.1007/s10021-017-0129-9, 2017.
Graven, H. D.: Impact of fossil fuel emissions on atmospheric radiocarbon and various applications of radiocarbon over this century, Proc. Natl. Acad. Sci., (Early Edition), 1–4, doi:10.1073/pnas.1504467112, 2015a.
Graven, H. D.: Impact of fossil fuel emissions on atmospheric radiocarbon and various applications of radiocarbon over this century, Proc. Natl. Acad. Sci., (Early Edition), 1–4, doi:10.1073/pnas.1504467112, 2015b.
Hagedorn, F., Bucher, J. B. and Schleppi, P.: Contrasting dynamics of dissolved inorganic and organic nitrogen in soil and surface waters of forested catchments with Gleysols, Geoderma, 100(1–2), 173–192, doi:10.1016/S0016-7061(00)00085-9, 2001a.
Hagedorn, F., Maurer, S., Egli, P., Blaser, P., Bucher, J. B. and Siegwo: Carbon sequestration in forest soils : effects of soil type , atmospheric CO 2 enrichment , and N deposition, Eur. J. Soil Sci., 52(December), 2001b.
Hagedorn, F., Saurer, M. and Blaser, P.: A 13C tracer study to identify the origin of dissolved organic carbon in forested mineral soils, Eur. J. Soil Sci., 55(1), 91–100 [online] Available from: http://doi.wiley.com/10.1046/j.1365-2389.2003.00578.x (Accessed 26 September 2013), 2004.
He, Y., Trumbore, S. E., Torn, M. S., Harden, J. W., Vaughn, L. J. S., Allison, S. D. and Randerson, J. T.: Radiocarbon constraints imply reduced carbon uptake by soils during the 21st century, Science (80-.)., 353(6306), 1419–1424, 2016.
Helfrich, M., Flessa, H., Mikutta, R., Dreves, A. and Ludwig, B.: Comparison of chemical fractionation methods for isolating stable soil organic carbon pools, Eur. J. Soil Sci., 58(6), 1316–1329, doi:10.1111/j.1365-2389.2007.00926.x, 2007.
Hemingway, J.: Microbial oxidation of lithospheric organic carbon in rapidly eroding tropical mountain soils, Science (80-.)., (April), doi:10.1126/science.aao6463, 2018.
Herold, N., Schöning, I., Michalzik, B., Trumbore, S. E. and Schrumpf, M.: Controls on soil carbon storage and turnover in German landscapes, Biogeochemistry, 119(1–3), 435–451, doi:x, 2014.
Hua, Q., Barbetti, M. and Rakowski, A. Z.: Atmospheric radiocarbon for the period 1950–2010, Radiocarbon, 55(4), 2059–2072, 2013.
Ivy-Ochs, S., Kerschner, H., Maisch, M., Christl, M., Kubik, P. W. and Schluchter, C.: Latest Pleistocene and Holocene glacier variations in the European Alps, Quat. Sci. Rev., 28(21–22), 2137–2149, doi:10.1016/j.quascirev.2009.03.009, 2009.
Jobbagy, E. G. and Jackson, R. .: Ther vertical distribution of soil organic carbon an its relation to climate and vegetation, Ecol. Appl., 10(April), 423–436, 2000.
Kaiser, K. and Kalbitz, K.: Cycling downwards - dissolved organic matter in soils, Soil Biol. Biochem., 52, 29–32, doi:10.1016/j.soilbio.2012.04.002, 2012.

546 Keiluweit, M., Bougoure, J. J., Nico, P. S., Pett-Ridge, J., Weber, P. K. and Kleber, M.: Mineral protection of
547 soil carbon counteracted by root exudates, Nat. Clim. Chang., 5(6), doi:10.1038/nclimate2580, 2015.
548 Klute, A.: Methods of soil analysis, Part 1: Physical and Mineralogical Methods, 2nd ed., Agronomy
549 Monograph No 9, Madison WI., 1986.
550 Koarashi, J., Hockaday, W. C., Masiello, C. a. and Trumbore, S. E.: Dynamics of decadally cycling carbon in
551 subsurface soils, J. Geophys. Res. Biogeosciences, 117(3), 1–13, doi:10.1029/2012JG002034, 2012.
552 Komada, T., Anderson, M. R. and Dorfmeier, C. L.: Carbonate removal from coastal sediments for the
553 determination of organic carbon and its isotopic signatures , δ 13 C and Δ 14 C : comparison of fumigation and
554 direct acidification by hydrochloric acid, Limnol. Oceanogr. Methods, (6), 254–262, 2008.
555 Lang, S. Q., McIntyre, C. P., Bernasconi, S. M., Früh-Green, G. L., Voss, B. M., Eglinton, T. I. and Wacker, L.:
556 Rapid 14C Analysis of Dissolved Organic Carbon in Non-Saline Waters, Radiocarbon, 58(3), 1–11,
557 doi:10.1017/RDC.2016.17, 2016.
558 Lechleitner, F. A., Baldini, J. U. L., Breitenbach, S. F. M., Fohlmeister, J., McIntyre, C., Goswami, B.,
559 Jamieson, R. A., van der Voort, T. S., Prufer, K., Marwan, N., Culleton, B. J., Kennett, D. J., Asmerom, Y.,
560 Polyak, V. and Eglinton, T. I.: Hydrological and climatological controls on radiocarbon concentrations in a
561 tropical stalagmite, Geochim. Cosmochim. Acta, doi:10.1016/j.gca.2016.08.039, 2016.
562 Lutzow, M. V, Kogel-Knabner, I., Ekschmitt, K., Matzner, E., Guggenberger, G., Marschner, B. and Flessa, H.:
563 Stabilization of organic matter in temperate soils: mechanisms and their relevance under different soil
564 conditions - a review, Eur. J. Soil Sci., 57, 426–445 [online] Available from:
565 http://doi.wiley.com/10.1111/j.1365-2389.2006.00809.x, 2006.
566 McFarlane, K. J., Torn, M. S., Hanson, P. J., Porras, R. C., Swanston, C. W., Callaham, M. A. and Guilderson,
567 T. P.: Comparison of soil organic matter dynamics at five temperate deciduous forests with physical
568 fractionation and radiocarbon measurements, Biogeochemistry, 112(1–3), 457–476, doi:10.1007/s10533-012-
569 9740-1, 2013.
570 Manzoni, S., Katul, G. G. and Porporato, A.: Analysis of soil carbon transit times and age distributions using
571 network theories, J. Geophys. Res. Biogeosciences, 114(4), 1–14, doi:10.1029/2009JG001070, 2009.
572 Mathieu, J. A., Hatté, C., Balesdent, J. and Parent, É.: Deep soil carbon dynamics are driven more by soil type
573 than by climate: A worldwide meta-analysis of radiocarbon profiles, Glob. Chang. Biol., 21(11), 4278–4292,
574 doi:10.1111/gcb.13012, 2015.
575 McIntyre, C. P., Wacker, L., Haghipour, N., Blattmann, T. M., Fahrni, S., Usman, M., Eglinton, T. I. and Synal,
576 H.-A.: Online 13C and 14C Gas Measurements by EA-IRMS–AMS at ETH Zürich, Radiocarbon,
577 002(November 2015), 1–11, doi:10.1017/RDC.2016.68, 2016.
578 Melillo, J. M., Steudler, P. a, Aber, J. D., Newkirk, K., Lux, H., Bowles, F. P., Catricala, C., Magill, A., Ahrens,
579 T. and Morrisseau, S.: Soil warming and carbon-cycle feedbacks to the climate system., Science, 298(5601),
580 2173–6 [online] Available from: http://www.ncbi.nlm.nih.gov/pubmed/12481133 (Accessed 21 January 2014),
581 2002.
582 Mills, R. T. E., Tipping, E., Bryant, C. L. and Emmett, B. a.: Long-term organic carbon turnover rates in natural
583 and semi-natural topsoils, Biogeochemistry, 118(1), 257–272 [online] Available from:
584 http://link.springer.com/10.1007/s10533-013-9928-z (Accessed 18 December 2013a), 2013.
585 Mills, R. T. E., Tipping, E., Bryant, C. L. and Emmett, B. a.: Long-term organic carbon turnover rates in natural
586 and semi-natural topsoils, Biogeochemistry, 118(1), 257–272 [online] Available from:
587 http://link.springer.com/10.1007/s10533-013-9928-z, 2013b.
588 Nussbaum, M., Papritz, A., Baltensweiler, A. and Walthert, L.: Estimating soil organic carbon stocks of Swiss
589 forest soils by robust external-drift kriging, Geosci. Model Dev., 7(3), 1197–1210, doi:10.5194/gmd-7-1197-
590 2014, 2014.
591 Paul, E. A., Collins, H. P. and Leavitt, S. W.: Dynamics of resistant soil carbon of midwestern agricultural soils
592 measured by naturally occurring 14C abundance, Geoderma, 104(3–4), 239–256, doi:10.1016/S0016-
593 7061(01)00083-0, 2001.
594 Paul, E. A., Follett, R. F., Leavitt, W. S., Halvorson, A., Petersen, G. A. and Lyon, D. J.: Radiocarbon Dating
595 for Determination of Soil Organic Matter Pool Sizes and Dynamics, Soil Sci. Soc. Am. J., 61(4), 1058–1067,
596 1997.
597 Prietzel, J., Zimmermann, L., Schubert, A. and Christophel, D.: Organic matter losses in German Alps forest
598 soils since the 1970s most likely caused by warming, Nat. Geosci., 9(July), doi:10.1038/ngeo2732, 2016.
599 Prior, C. A., Baisden, W. T., Bruhn, F. and Neff, J. C.: Using a soil chronosequence to identify soil fractions for
600 understanding and modeling soil carbon dynamics in New Zealand, Radiocarbon, 49(2), 1093–1102, 2007.
601 Rasse, D. P., Rumpel, C. and Dignac, M.-F.: Is soil carbon mostly root carbon? Mechanisms for a specific
602 stabilisation, Plant Soil, 269(1–2), 341–356 [online] Available from: http://link.springer.com/10.1007/s11104-
603 004-0907-y, 2005.
604 Rethemeyer, J., Kramer, C., Gleixner, G., John, B., Yamashita, T., Flessa, H., Andersen, N., Nadeau, M. and
605 Grootes, P. M.: Transformation of organic matter in agricultural soils : radiocarbon concentration versus soil

depth, Geoderma, 128, 94–105, doi:10.1016/j.geoderma.2004.12.017, 2005.
Richter, D. D. and Markewitz, D.: Understanding Soil Change, Cambridge University Press, Cambridge., 2001.
Rumpel, C. and Kogel-Knabner, I.: Deep soil organic matter—a key but poorly understood component of terrestrial C cycle, Plant Soil, 338, 143–158, 2011a.
Rumpel, C. and Kogel-Knabner, I.: Deep soil organic matter—a key but poorly understood component of terrestrial C cycle, Plant Soil, 338, 143–158, 2011b.
Sanderman, J. and Amundson, R.: A comparative study of dissolved organic carbon transport and stabilization in California forest and grassland soils, Biogeochemistry, 92(1–2), 41–59, doi:10.1007/s10533-008-9249-9, 2009.
Scharpenseel, H. W. and Becker-Heidelmann, P.: Shifts in 14C patterns of soil profiles due to bomb carbon, including effects of morphogenetic and turbation processes, Radiocarbon, 31(3), 627–636, 1989.
Schaub, M., Dobbertin, M., Kräuchi, N. and Dobbertin, M. K.: Preface-long-term ecosystem research: Understanding the present to shape the future, Environ. Monit. Assess., 174(1–4), 1–2, doi:10.1007/s10661-010-1756-1, 2011.
Schimel, D. S., House, J. I., Hibbard, K. a, Bousquet, P., Ciais, P., Peylin, P., Braswell, B. H., Apps, M. J., Baker, D., Bondeau, A., Canadell, J., Churkina, G., Cramer, W., Denning, a S., Field, C. B., Friedlingstein, P., Goodale, C., Heimann, M., Houghton, R. a, Melillo, J. M., Moore, B., Murdiyarso, D., Noble, I., Pacala, S. W., Prentice, I. C., Raupach, M. R., Rayner, P. J., Scholes, R. J., Steffen, W. L. and Wirth, C.: Recent patterns and mechanisms of carbon exchange by terrestrial ecosystems., Nature, 414(6860), 169–72 [online] Available from: http://www.ncbi.nlm.nih.gov/pubmed/11700548, 2001.
Schleppi, P., Muller, N., Feyen, H., Papritz, A., Bucher, J. B. and Fluehler, H.: Nitrogen budgets of two small experimental forested catchments at Alptal , Switzerland, For. Ecol. Manage., 127(101), 177–185, 1998.
Schmidt, M. W. I., Torn, M. S., Abiven, S., Dittmar, T., Guggenberger, G., Janssens, I. a, Kleber, M., Kögel-Knabner, I., Lehmann, J., Manning, D. a C., Nannipieri, P., Rasse, D. P., Weiner, S. and Trumbore, S. E.: Persistence of soil organic matter as an ecosystem property., Nature, 478(7367), 49–56 [online] Available from: http://www.ncbi.nlm.nih.gov/pubmed/21979045 (Accessed 21 January 2014), 2011.
Schrumpf, M. and Kaiser, K.: Large differences in estimates of soil organic carbon turnover in density fractions by using single and repeated radiocarbon inventories, Geoderma, 239–240, 168–178 [online] Available from: http://linkinghub.elsevier.com/retrieve/pii/S0016706114003577, 2015.
Schrumpf, M., Kaiser, K., Guggenberger, G., Persson, T., Kogel-Knabner, I. and Schulze, E.-D.: Storage and stability of organic carbon in soils as related to depth , occlusion within aggregates , and attachment to minerals, Biogeosciences, 10, 1675–1691, 2013.
Seneviratne, S. I., Corti, T., Davin, E. L., Hirschi, M., Jaeger, E. B., Lehner, I., Orlowsky, B. and Teuling, A. J.: Investigating soil moisture-climate interactions in a changing climate: A review, Earth-Science Rev., 99(3–4), 125–161, doi:10.1016/j.earscirev.2010.02.004, 2010.
Sierra, C. A., Muller, M., Metzler, H., Manzoni, S. and Trumbore, S. E.: The muddle of ages, turnover, transit, and residence times in the carbon cycle, Glob. Chang. Biol., 1–11, doi:10.1111/gcb.13556, 2016.
Smith, J. C., Galy, A., Hovius, N., Tye, A. M., Turowski, J. M. and Schleppi, P.: Runoff-driven export of particulate organic carbon from soil in temperate forested uplands, Earth Planet. Sci. Lett., 365, 198–208, doi:10.1016/j.epsl.2013.01.027, 2013.
Solly, E., Schöning, I., Boch, S., Müller, J., Socher, S. a., Trumbore, S. E. and Schrumpf, M.: Mean age of carbon in fine roots from temperate forests and grasslands with different management, Biogeosciences, 10(7), 4833–4843, doi:10.5194/bg-10-4833-2013, 2013.
Torn, M. S., Swanston, C. W., Castanha, C. and Trumbore, S. E.: Storage and turnover of organic matter in soil, in Biophysico-Chemical Processes Involving Natural Nonliving Organic Matter in Environmental Systems, edited by N. Senesi, B. Xing, and P. M. Huang, p. 54, John Wiley & Sons, Inc., 2009.
Trumbore, S. E. and Czimczik, C. I.: Geology. An uncertain future for soil carbon., Science, 321, 1455–1456, 2008.
van der Voort, T. S., Hagedorn, F., Mcintyre, C., Zell, C., Walthert, L. and Schleppi, P.: Variability in 14 C contents of soil organic matter at the plot and regional scale across climatic and geologic gradients, Biogeosciences, 13(January), 3427–3439, doi:10.5194/bg-2015-649, 2016.
Wacker, L., Bonani, G., Friedrich, M., Hajdas, I., Kromer, B., NĬmec, M., Ruff, M., Suter, M., Synal, H.-A. and Vockenhuber, C.: MICADAS: Routine and high-precision radiocarbon dating, Radiocarbon, 52(2), 252–262, 2010.
Wacker, L., Němec, M. and Bourquin, J.: A revolutionary graphitisation system: Fully automated, compact and simple, Nucl. Instruments Methods Phys. Res. Sect. B Beam Interact. with Mater. Atoms, 268(7–8), 931–934 [online] Available from: http://linkinghub.elsevier.com/retrieve/pii/S0168583X09011161 (Accessed 2 August 2013), 2009.
Walthert, L., Blaser, P., Lüscher, P., Luster, J. and Zimmermann, S.: Langfristige Waldökosystem-Forschung LWF in der Schweiz. Kernprojekt Bodenmatrix. Ergebnisse der ersten Erhebung 1994–1999., 2003.

Walthert, L., Graf Pannatier, E. and Meier, E. S.: Shortage of nutrients and excess of toxic elements in soils limit the distribution of soil-sensitive tree species in temperate forests, For. Ecol. Manage., 297, 94–107, doi:10.1016/j.foreco.2013.02.008, 2013.
Walthert, L., Lüscher, P., Luster, J. and Peter, B.: Langfristige Waldökosystem- Forschung LWF. Kernprojekt Bodenmatrix. Aufnahmeanleitung zur ersten Erhebung 1994–1999, Swiss Federal Institute for Forest, Snow and Landscape Research WSL, Birmensdorf., 2002a.
Walthert, L., Lüscher, P., Luster, J. and Peter, B.: Langfristige Waldökosystem-Forschung LWF in der Schweiz. Kernprojekt Bodenmatrix. Aufnahmeanleitung zur ersten Erhebung 1994–1999, Birmensdorf. [online] Available from: http://e-collection.ethbib.ethz.ch/show?type=bericht&nr=269, 2002b.

Author contributions

T.S. van der Voort planned, coordinated and executed the sampling strategy and sample collection, performed the analyses, conceptualized and optimized the model and processed resulting data. U. Mannu led the model development. F. Hagedorn lent his expertise on soil carbon cycling and soil properties. C. McIntyre facilitated and coordinated the radiocarbon measurements and associated data corrections. L. Walthert and P. Schleppi lent their expertise on the legacy sampling and provided data for the compositional analysis. N. Haghipour performed in isotopic and compositional measurements. T. Eglinton provided the conceptual framework and aided in the paper structure set-up. T.S. van der Voort prepared the manuscript with help of all co-authors.

Tables

Table 1 Overview sampling locations and climatic and ecological parameters.

Location	Soil type	Geology	Latitude(N)/ Longitude (E)	Soil depth (m)	Depth Upper limit waterlogging (m)[1]	Altitude Elevation (m a.s.l.)	MAT °C	MAP mm y^{-1}	NPP g C $m^{-2}y^{-1}$
Othmarsingen[1, 2, 3]	Luvisol	Calcareous moraine	47°24'/8°14'	>1.9	2.5	467-500	9.2	1024	845
Lausanne[1, 2, 3]	Cambisol	Calcarous and shaly moraine	46°34'/6°39'	>3.2	2.5	800-814	7.6	1134	824
Alptal[1, 2, 3, 4]	Gleysol	Flysch (carbon-holding sedimentary rock)	47°02'/8°43'	>1.0	0.1	1200	5.3	2126	347
Beatenberg[1, 2, 3]	Podzol	Sandstone	46°42'/7°46'	0.65	0.5	1178-1191	4.7	1163	302
Nationalpark[1, 2, 3]	Fluvisol	Calcareous alluvial fan	46°40'/10°14'	>1.1	2.5	1890-1907	1.3	864	111

[1] Walthert et al. (2003) [2]Etzold et al., (2014) [3]Von Arx et al., (2013) [4]Krause et al., (2013) for Alptal data

Table 2 Vegetation and soil data of the study sites. Soil water potential (hPa) are for 15 cm depth.

Location[1]	Deciduous tree species (%)[3]	Dominant tree species[3]	Inferred lag carbon fixation (y)	Organic layer Type[1]	Soil water potential (hPa) percentiles[3]		
					5%	50%	95%
Othmarsingen	100	*Fagus sylvatica*	2	Mull	-577	-39	-9
Lausanne	80	*Fagus sylvatica*	3	Mull	-547	-49	-8
Alptal[4]	15	*Picea abies*	7	Mor to anmoor	-38	-13	+1
Beatenberg	0	*Picea abies*	8	Mor	-50	-14	+1
Nationalpark	0	*Pinus montana*	8	Moder	-388	-65	-13

[1] Walthert et al. (2003) [2]Etzold et al., (2014), [3]Von Arx et al. (2013),[4]Krause et al., (2013)

Table 3 Soil properties as well as carbon stocks and fluxes in 0-20, 20-60, and 60-100 cm depth of the study sites for the bulk and water-extractable organic carbon (WEOC).

Location	Depth interval (m)	pH[1]	CEC[1](mmolc/kg)	$Fe_{exchangeable}$ (mmolc/kg)	$Al_{exchangeable}$ (mmolc/kg)	Sand content (%)	Silt content (%)	Clay content (%)	Carbon stock kgC/m^2	Average turnover bulk (y)	Average turnover WEOC (y)
Othmarsingen[1]	0.0-0.2	4.4	62.2	0.15	42	46.8	35.5	17.6	4.84	173	35
	0.2-0.6	4.4	62.8	0.10	49	44.3	33.3	22.4	1.69	868	518
	0.6-0.8	4.9	99.5	0.06	41	46.7	28.4	25.0	0.28	3938	-
Lausanne[1]	0.0-0.2	4.5	60.8	0.13	43	49.2	32.6	18.2	3.24	353	77
	0.2-0.6	4.6	43.9	0	34	50.2	32.0	17.8	2.12	1239	588
	0.6-1.0	4.8	49.7	0	35	50.5	31.5	18.1	0.69	2246	1502[5]
Alptal[2,3,4]	0.0-0.2	4.5	417	-	19	19.3	39.4	41.3	7.73	437	162
	0.2-0.6	4.7	340	-	14	4.90	47.0	48.1	7.24	3314	893[6]
	0.6-1.0	4.7	340	-	-	-	-	-	6.54	5165	-
Beatenberg[1]	Organic layer	3.1	260.2	2.8	33	-	-	-	7.05	53	-
	0.0-0.2	4.0	35.6	1.7	18	84.9	12.4	2.7	3.65	1224	293
	0.2-0.6	4.1	23.1	0.40	17	83.2	12.3	4.6	4.10	1607	677
Nationalpark[1]	0.0-0.2	8.3	171.8	0.1	0.0	47.5	34.8	17.7	3.23	180	92
	0.2-0.6	8.8	106.3	0.0	0.0	61.9	32.5	5.7	0.36	612	214
	0.6-0.8	-	-	0.0	0.0	60.6	33.6	5.9	0.08	983	-

[1]Walthert et al., 2002, Walthert et al., 2003., Fe and Al content (mmolc/kg) determined by NH_4Cl extraction.
For the 0.2-0.6 depth interval the CEC determined for 0.2-0.4 m was taken, and similarly for the depth interval 0.6-1.0 m the values for 0.6-0.8 m were taken in the case of Othmarsingen, Lausanne Beatenberg and Nationalpark.
[2]Krause et al., 2013
[3]Diserens et al,1992, CEC determined (mmeq/kg), hydrogen lead and zinc ions were not included, Aluminium content determined by Lakanen method. CEC values for 0.2-0.4 m were extrapolated to 1 m. [4]Xu et al., 2009 [5]Depth to 0.8 m [6]Depth to 0.4 m

Table 4 Pearson correlations for averaged depth intervals for the top soil (0-20 cm, n=5) and deep soil (20-60 cm, n=5). Significance denoted with **˙,** *, ** or *** for respectively p-values smaller than 0.1 (marginally significant) 0.05, 0.005 and 0.0005 (significant). Non-significant correlations are indicated by the superscript **ns**. SWP or soil water potential used are the median values at 15 cm for each of these 5 sites (Von Arx et al., 2013). Water-extractable carbon is abbreviated to WEOC. Results indicate that no single climatic or textural factor consistently co-varies with carbon stocks, or turnover time.

Explaining variable	**Stock$_{0\text{-}20\ cm}$**	**Turnover time bulk$_{0\text{-}20\ cm}$**	**Turnover time WEOC $_{0\text{-}20\ cm}$**	**Stock$_{20\text{-}60\ cm}$**	**Turnover time$_{20\text{-}60\ cm}$**
MAT	0.17^{ns}	-0.14^{ns}	-0.36^{ns}	0.02^{ns}	0.02^{ns}
MAP	**0.96***	0.11^{ns}	0.28^{ns}	**0.93***	**0.98****
NPP	0.2^{ns}	0.65^{ns}	0.39^{ns}	0.03^{ns}	-0.10^{ns}
Sand	-0.66^{ns}	0.72^{ns}	0.55^{ns}	-0.56^{ns}	-0.70^{ns}
Silt	0.38^{ns}	**-0.91***	-0.79^{ns}	0.29^{ns}	-0.47^{ns}
Clay	**0.81˙**	-0.51^{ns}	-0.31^{ns}	0.71^{ns}	0.80^{ns}
CEC	-0.67^{ns}	-0.24^{ns}	0.03^{ns}	0.74^{ns}	**0.82˙**
pH	-0.74^{ns}	-0.47^{ns}	-0.31^{ns}	-0.51^{ns}	-0.46^{ns}
Fe	0.24^{ns}	0.98*	0.97*	0.98*	-0.78^{ns}
Al	0.18^{ns}	-0.16^{ns}	-0.41^{ns}	-0.17^{ns}	-0.17^{ns}
SWP	0.70^{ns}	0.68^{ns}	0.70^{ns}	-	-
Average Grain size	-0.25^{ns}	**0.97***	**0.88˙**	0.05^{ns}	-0.16^{ns}

Figures

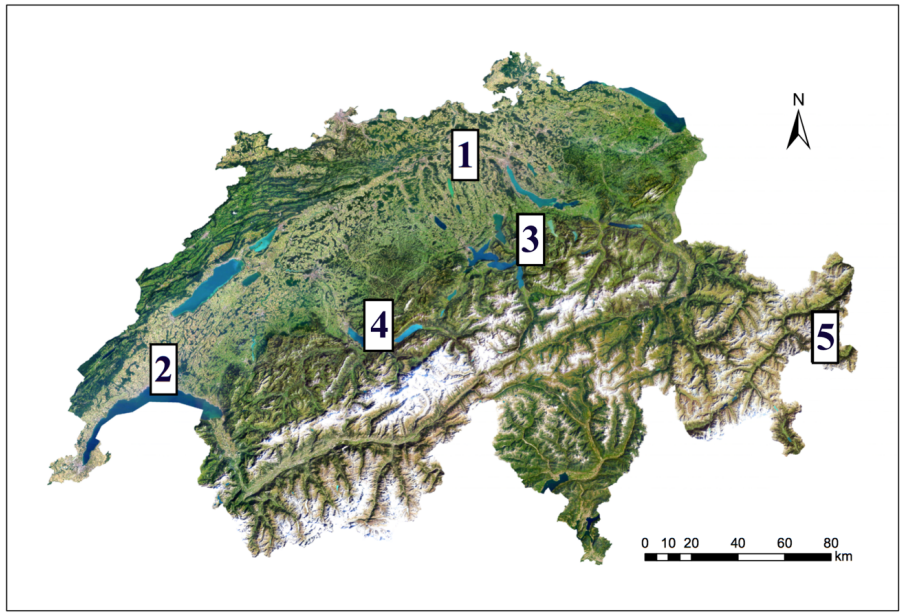

Figure 1 Sample locations, all of which are part of the Long-term ecosystem research program (LWF) of the Swiss Federal Institute WSL, 1) Othmarsingen, 2) Lausanne, 3) Alptal, 4) Beatenberg and 5) Nationalpark Image made using 2016 swisstopo (JD100042).

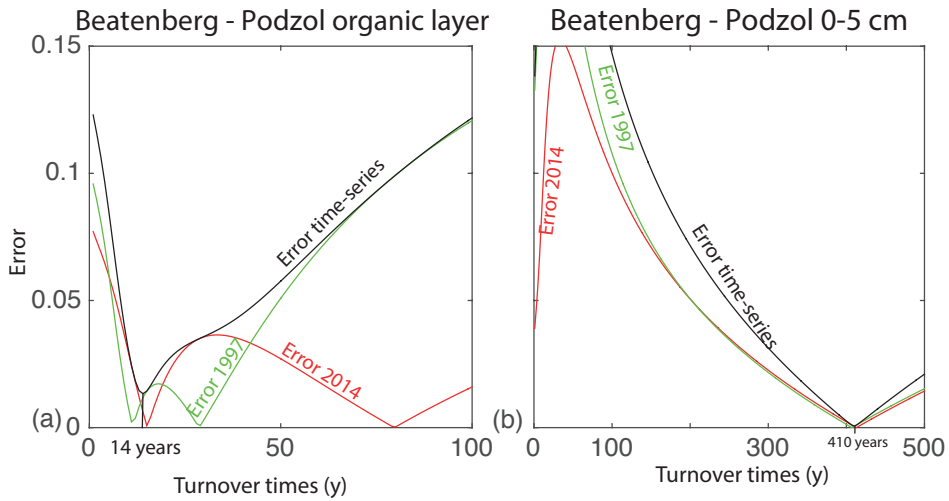

Figure 2 Numerical optimization of least mean-square error reduction, showing and the reduction of error spread for two soil depths. For the Beatenberg Podzol organic layer (a) the individual ^{14}C time-points for both 1997 and 2014 both yield two solutions are almost equally likely (i.e. the error nears zero). The combined optimization using both the time-points reveal the likeliest option. For the (b) 0-5 cm layer the single time points only have a single likely solution.

Comment [TSvdV4]: Figure also augmented with soil type as suggested

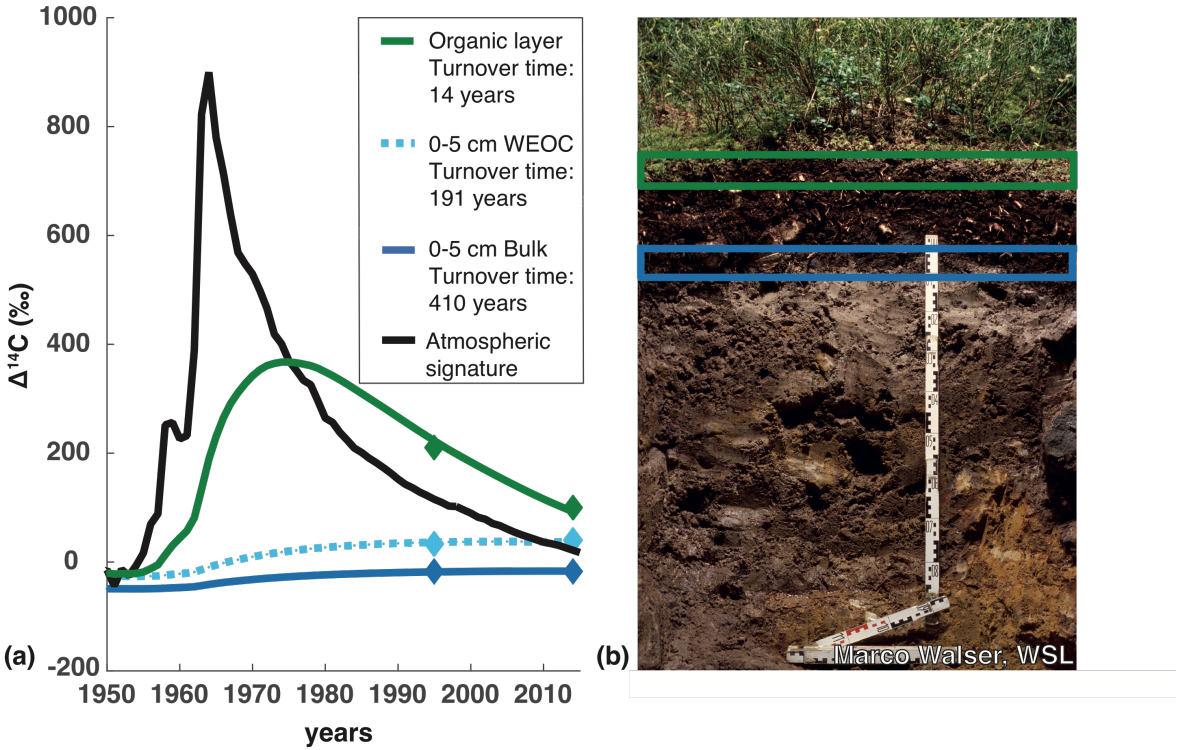

Figure 3 (a) Time-series soil carbon turnover time in years (y) as determined by numerical modelling for (b) sub-alpine site Podzol Beatenberg. The bulk turnover in the organic layer is rapid (14 years), followed by the turnover of the water-extractable organic carbon (WEOC) (191 years) and the bulk turnover of the soil (410 years). Photo soil profile courtesy of Marco Walser, WSL.

Comment [TSvdV5]: Figure also augmented with soil type as suggested

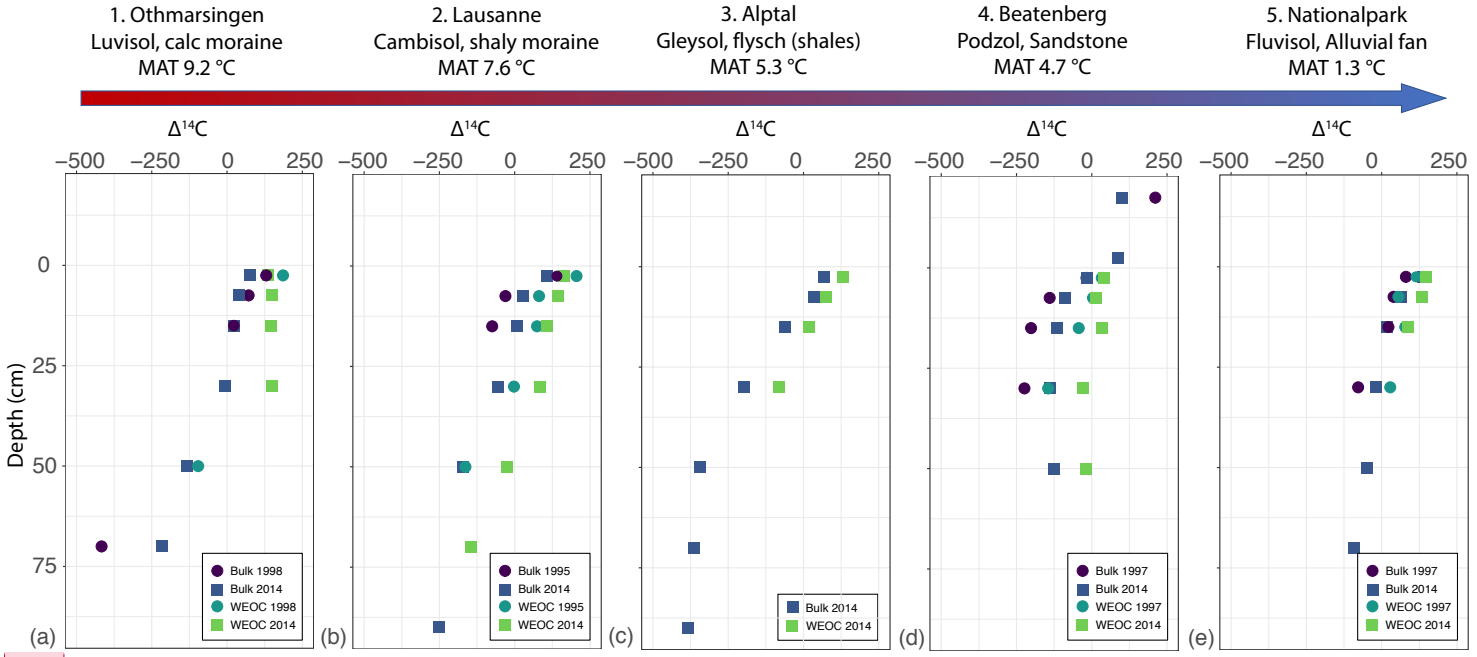

Figure 4 (a-e) Changes in radiocarbon signature of both bulk soil and WEOC over two decades at four sites on a climatic gradient. For Alptal (Gleysol) (c) only the 2014 time-point was available. For the warmer locations Othmarsingen and Lausanne (Luvisol, Cambisol MAT 9.2-7.6 °C), depletion in bomb-derived radiocarbon occurs in the first five centimeters soil in 2014 as compared to 1995-8. The colder Beatenberg site (Podzol, MAT 4.7 °C) is marked by a clear enrichment of ^{14}C in the mineral soil in 2014 w.r.t. 1997. At the coldest site Nationalpark (Fluvisol, MAT 1.3 °C) almost all samples taken two decades after the initial sampling show an enrichment in radiocarbon signature. WEOC contains bomb-derived carbon in the topsoil in 2014 at all sites.

Comment [TSvdV6]: Dear Sébastian, as suggested we have now included the soil types both in the figure heading as well as the text. We have improved the text following this suggestion elsewhere as well. We have also augmented the colours in this figure as compared to the previous version.

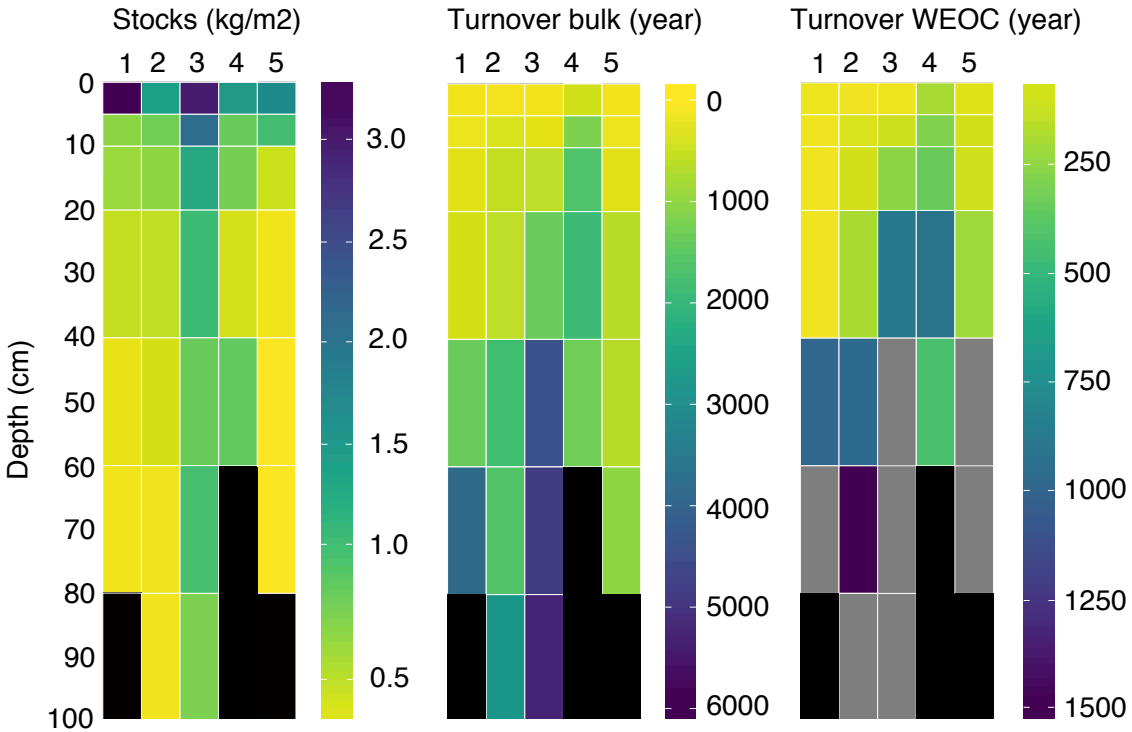

Figure 5 Carbon (a) stocks in the mineral soil kgC/m^2, (b) turnover time bulk soil in years and (c) turnover time water extractable organic carbon soil in years. Locations are ordered from the warmest to coldest sites i.e. (1) Othmarsingen (Luvisol), (2) Lausanne (Cambisol), (3) Alptal (Gleysol), (4) Beatenberg (Podzol) and (5) Nationalpark (Fluvisol). Grey boxes indicate absence of material, black boxes indicate the occurence of the C-horizon (poorly consolidated bedrock-derived stony material or bedrock itself).

Comment [TSvdV7]: Figure also augmented with soil type as suggested

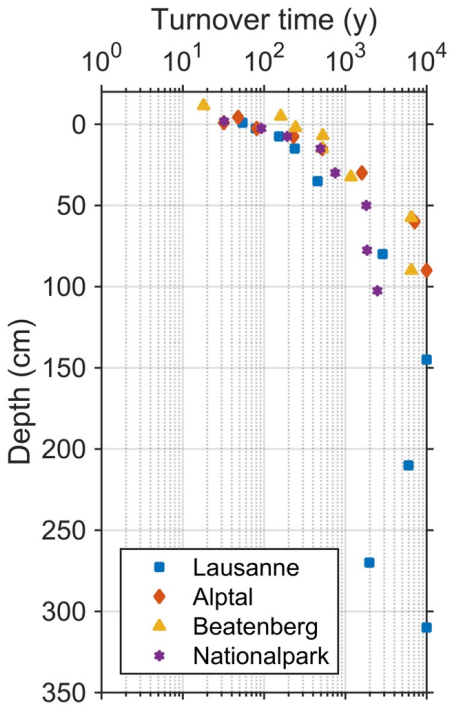

Figure 6 Modeled turnover times (y) of single profiles sampled down to the bedrock between 1995 and 1998. $\Delta^{14}C$ published in Van der Voort et al. (2016). Results indicate presence of petrogenic (bedrock-derived) carbon as modeled turnover time exceeds soil formation since the end of last ice age (10,000 years) in Lausanne (>100 cm, Cambisol) and Alptal (80-100 cm, Gleysol). For Beatenberg (Podzol) and Nationalpark (Fluvisol), no petrogenic carbon was found.